Continuum percolation and pair-connectedness function in binary mixtures of strongly interacting particles

1989 J. Phys. A: Math. Gen. 22 3969

(http://iopscience.iop.org/0305-4470/22/18/030)

J. Phys. A: Math. Gen. **22** (1989) 3969-3979. Printed in the UK

Continuum percolation and pair-connectedness function in binary mixtures of strongly interacting particles

Yee C Chiew† and Eduardo D Glandt‡

† Department of Chemical and Biochemical Engineering, Rutgers University, Piscataway, NJ 08855-0909, USA

‡ Department of Chemical Engineering, University of Pennsylvania, Philadelphia, PA 19104-6393, USA

Received 8 March 1989

Abstract. We study continuum percolation and aggregation in binary mixtures of strongly interacting particles. The clustering and connectivity behaviour of the dispersed particles are determined using the Ornstein-Zernike integral equation in the Percus-Yevick (PY) integral equation. Specifically, we consider a binary mixture of spheres in which the interactions between like species are strongly attractive, while the interaction between unlike species is purely repulsive. We model this system through hard-core square-well (SW) potentials, which we approximate by the adhesive hard-sphere model, which yields analytic solutions in the PY theory. We derive the general solution for the percolation behaviour of a binary mixture of adhesive hard spheres. We report analytic results for the system of interest: the percolation threshold, the average size of the clusters and the pair-connectedness functions in terms of temperature, particle-size ratio, composition and particle densities. We find that the repulsion between unlike species enhances the clustering of the particles.

1. Introduction

A great deal of effort has been directed toward the study of the percolation and clustering behaviour of dispersions of strongly interacting particles, e.g. colloids, microemulsions, etc. Experimental measurements of the conductivity of microemulsions suggest that the percolation threshold in these systems not only depends on temperature and particle volume fraction, but also on the interparticle forces (Bhattacharya *et al* 1985, Cazabat *et al* 1984, Kim and Huang 1986). In particular, the behaviour of microemulsions has been successfully modelled by the hard-core square-well potential (Huang *et al* 1984). Theoretical and computer simulation studies on the percolation behaviour of hard-core square-well systems have also been reported in the literature (Safran *et al* 1985, Bug *et al* 1985, Netemeyer and Glandt 1986, Chiew and Wang 1988). In these studies, the effects of temperature, particle volume fraction, well depth, well width, and the connectivity distance on the percolation threshold were examined in detail. Also, the pair-connectedness function of the square-well fluid has been theoretically determined in the Percus-Yevick (PY) approximation (Netemeyer and Glandt 1986), and through Monte Carlo simulation (Chiew and Wang, 1988).

In the present work, however, we examine the percolation in *mixtures* of strongly interacting particles. Specifically we consider a binary mixture (consisting of species A and B) in which strong attraction is found among the like species (i.e. among the

0305-4470/89/183969+11$02.50

A-A and B-B pairs), while the interaction between the unlike particles is purely repulsive. Thus, particle clustering is found among the A or B particles only. Hence, the system may have one percolating cluster of particles (either of species A or B), or two simultaneously percolating clusters. We examine the effects of temperature, the repulsion between unlike species, particle volume fraction, particle sizes, and strength of attraction on the percolation behaviour of the mixture.

In this study, the percolation threshold of the mixture is determined through the connectivity Ornstein-Zernike (OZ) integral equation (Coniglio *et al* 1977). This approach has been employed to study a number of model systems; these include the randomly centred spheres, the permeable spheres (Chiew and Glandt 1983, Chiew *et al* 1985, Wu and Chiew 1989), the adhesive hard sphere (Chiew and Glandt 1983), the penetrable concentric shell model (DeSimone *et al* 1985), and the square-well fluids (Netemeyer and Glandt 1986). The OZ approach is based on the concept of physical clusters (Hill 1955). It is built around the pair-connectedness function $g_{ij}^{+}(r)$ which is defined so that $\rho_i \rho_j g_{ij}^{+}(\boldsymbol{r}_1, \boldsymbol{r}_2)\, d\boldsymbol{r}_1\, d\boldsymbol{r}_2$ represents the probability of finding a particle, of species i, situated in volume element $d\boldsymbol{r}_1$ at $\boldsymbol{r}_1$, and another particle, belonging to the same cluster, of species j, situated in volume element $d\boldsymbol{r}_2$ ar $\boldsymbol{r}_2$. It has been shown that the mixture pair-connectedness function $g_{ij}^{+}(r)$ is related to the so-called direct-connectedness function $c_{ij}^{+}(r)$ by the following Ornstein-Zernike equation (Chiew *et al* 1985):

$$g_{ij}^{+}(r) = c_{ij}^{+}(r) + \sum_k \rho_k \int c_{ij}^{+}(|\boldsymbol{s}|) g_{ij}^{+}(|\boldsymbol{r}-\boldsymbol{s}|)\, d\boldsymbol{s}. \tag{1}$$

Equation (1) can be solved subject to an appropriate closure. The most commonly used closure in this connection is the Percus-Yevick approximation (Coniglio *et al* 1977, Stell 1984). After determining the pair-connectedness function, the percolation threshold can be obtained by first computing the mean cluster size S using (Chiew *et al* 1985):

$$S = 1 + \rho \sum_i \sum_j x_i x_j \int g_{ij}^{+}(\boldsymbol{r})\, d\boldsymbol{r} \tag{2}$$

followed by taking the limit of $S \to \infty$ to yield the percolation threshold. In (2), $x_i = \rho_i / \Sigma_k \rho_k$ denotes the number fraction of species i.

2. The model

We consider a binary mixture (consisting of particles of species A and B) in which the interaction between the unlike species is repulsive, while mutual attraction is present between the like species. We model the strong attractive forces between the like species modelled by the hard-core square-well potential, while the interaction between species A and B is given by the hard-sphere potential, i.e. for $i = \mathrm{A}$ or $i = \mathrm{B}$, we have

$$\phi_{ii}(r) = \begin{cases} \infty & r < R_i \qquad (3a) \\ -\varepsilon_i & R_i < r < W_i R_i \qquad (3b) \\ 0 & r > W_i R_i \qquad (3c) \end{cases}$$

and

$$\phi_{AB}(r) = \begin{cases} \infty & r < R_{AB} \quad (4a) \\ 0 & r > R_{AB}. \quad (4b) \end{cases}$$

Here, R_i represents the hard-core diameter of species i; $R_{AB} = (R_A + R_B)/2$, $(W_i - 1)R_i$ denotes the width of the attractive square well, and ε_i is the depth of the well. As it stands, the square-well system, given by (3) and (4), does not yield analytic solutions in the PY closure. Our approach is to represent the square-well system by the simpler adhesive hard sphere (AHS) model, which can be solved analytically in the PY approximation. The Boltzmann factor $e_{ij}(r) = \exp(-\beta\phi_{ij}(r))$ of the AHS is given by

$$e_{ij}(r) = \begin{cases} \dfrac{R_{ij}}{12\tau_{ij}}\,\delta(r - R_{ij}) & 0 < r < R_{ij} \quad (5a) \\ 1 & r > R_{ij}. \quad (5b) \end{cases}$$

The mutual attraction between particles in the adhesive hard sphere model is characterised by a surface adhesiveness or 'stickiness' which is accounted for by the Dirac delta function in (5*a*). The quantitative measure of the strength of this stickiness is given by the parameter τ_{ij}^{-1}. The parameter τ_{ij} can also be viewed as a dimensionless indicator of the temperature of the system. It is noted that for the hard-sphere potential, $\tau_{ij} \to \infty$. A relationship between the adhesive hard spheres and the square-well system can be established by equating their respective second virial coefficients. For the system considered here, it is found that (for $i = A$ or B)

$$\tau_{ii}^{-1} = 4\{1 - [W_i^3 - \exp(\beta\varepsilon_i)(W_i^3 - 1)]\} \quad (6a)$$

and

$$\tau_{AB}^{-1} = 0. \quad (6b)$$

The 'stickiness' parameter τ_{AB}^{-1} is set to zero because the interaction between the A and B particles is of the hard-sphere type. An examination of (6*a*) and (6*b*) shows that, for fixed values of ε_i and W_i, τ_{ii} ($i = A$ or B) increases with the absolute temperature T. On the other hand, at a fixed temperature T, τ_{ii} decreases with increasing ε_i and W_i (i.e. the overall strength of attraction). In what follows, we shall consider τ_{AA} to be a dimensionless indicator of temperature T, while τ_{BB} will be taken as an integral measure of the strength of attraction between the type-B particles at the temperature specified by τ_{AA}.

In the study of the physical clustering of particles (Hill 1955), the Boltzmann factor $e_{ij}(r)$ is separated into its connected and non-connected parts, represented by $e_{ij}^{+}(r)$ and $e_{ij}^{*}(r)$, respectively, so that $e_{ij}(r) = e_{ij}^{+}(r) + e_{ij}^{*}(r)$. Similarly, the Mayer function $f_{ij}(r) = e_{ij}(r) - 1$ can also be decomposed into its respective connected and non-connected parts, i.e.

$$f_{ij}^{+}(r) = e_{ij}^{+}(r) \quad (7a)$$

$$f_{ij}^{*}(r) = e_{ij}(r) - 1 - e_{ij}^{+}(r). \quad (7b)$$

The PY solution to the pair-connectedness function of the AHS mixture can be obtained by solving the OZ equation subject to the following closure (Stell 1984):

$$c_{ij}^{+} = f_{ij}^{+}[g_{ij} - c_{ij}] + f_{ij}^{*}[g_{ij}^{+} - c_{ij}^{+}] \quad (8)$$

where g_{ij} and c_{ij} represent the radial distribution function and the direct-correlation function, respectively. Combining equations (5), (7) and (8) gives the boundary conditions to the OZ equation

$$g_{ij}^{+}(r) = g_{ij}(r) = \frac{\lambda_{ij} R_{ij}}{12}\,\delta(r - R_{ij}) \qquad 0 < r < R_{ij} \tag{9a}$$

$$c_{ij}^{+}(r) = 0 \qquad r > R_{ij} \tag{9b}$$

The parameter λ_{ij} in the coefficient of the Dirac delta function in (9*a*), accounts for the number of species-j particles that are in contact with a type-i particle. More precisely, the number of type-j particles that are in direct contact with a type-i particle, z_{ij}, is given by

$$z_{ij} = 2\lambda_{ij}\left(\frac{R_{ij}}{R_j}\right)^3 \eta_j. \tag{10}$$

The parameter λ_{ij} has been found to be a function of τ_{ij}, ρ_i and R_{ij}, given by (Cummings *et al* 1976, Perram and Smith 1977):

$$\lambda_{ij}\tau_{ij} = \frac{1}{(1-\xi_3)} + \frac{3\xi_2 R_i R_j/2}{(1-\xi_3)^2 R_{ij}} + \frac{\pi}{72 R_{ij}} \sum_k \rho_k \lambda_{ik}\lambda_{kj} R_{ik}^2 R_{kj}^2$$

$$- \frac{\pi}{12 R_{ij}(1-\xi_3)} \sum_k \rho_k R_k (\lambda_{ik} R_i R_{ik}^2 + \lambda_{kj} R_i R_{kj}^2) \tag{11}$$

where $\xi_m = (\pi/6)\,\Sigma_k\, \rho_k R_k^m$. Note that $\lambda_{AB} = 0$ for the system considered here, because there is no attraction between unlike species.

3. PY solution of the connectivity problem

The connectivity OZ equation (1) can be solved analytically in the PY approximation through the use of Baxter's factorisation technique (Baxter 1968a, b). In this method, the connectedness function $g_{ij}^{+}(r)$ can be shown to follow

$$r g_{ij}^{+}(r) = -q_{ij}'(r) + 2\pi \sum_k \rho_k \int_{S_{ij}}^{R_{ij}} \mathrm{d}t\, q_{ik}^{(t)}(r-t) g_{kj}^{+}(r-t). \tag{12}$$

Here, $S_{ij} = (R_i - R_j)/2$, and $q_{ij}(r)$ is a short-ranged function which vanishes for $r > R_{ij}$ and $r < S_{ij}$. Substituting (9*a*) into (11) yields

$$q_{ij}^{(r)} = \begin{cases} \dfrac{\lambda_{ij} R_{ij}^2}{12} & S_{ij} < r < R_{ij} \qquad (13a) \\ 0 & r > R_{ij}. \qquad (13b) \end{cases}$$

The Ornstein-Zernike integral equations can also be expressed in the following matrix form:

$$I + \tilde{G}(k) = [I - \tilde{C}(k)]^{-1} \tag{14}$$

where I is an identity matrix, and $\tilde{G}(k)$ and $\tilde{C}(k)$ are square matrices whose ijth

elements are, respectively, given by

$$\tilde{G}_{ij} = 4\pi\sqrt{(\rho_i\rho_j)}\, k^{-1} \int r g_{ij}^{+}(r) \sin kr \, dr \tag{15}$$

$$\tilde{C}_{ij} = 4\pi\sqrt{(\rho_i\rho_j)}\, k^{-1} \int r c_{ij}^{+}(r) \sin kr \, dr. \tag{16}$$

Baxter (1970) has shown that the function $q_{ij}^{(r)}$ is related to $\tilde{G}(k)$ by

$$I + \tilde{G}(k) = [\tilde{Q}^{T}(-k)\tilde{Q}(k)]^{-1} \tag{17}$$

where the ijth element of the matrix $\tilde{Q}(k)$ is given by

$$\tilde{Q}_{ij} = \delta_{ij} - 2\pi\sqrt{(\rho_i\rho_j)} \int_{s_{ij}}^{R_{ij}} q_{ij}(r) \exp(ikr)\, dr. \tag{18}$$

Combining (2), (13), (15), (17) and (18) yields the following expression for the average particle-cluster size S:

$$S = \frac{1}{\Delta^2}\left[x_A \left((1-\lambda_{BB}\eta_B) + \frac{\pi}{6}\rho_B\lambda_{AB}R_A R_{AB}^2 \right)^2 + x_B \left((1-\lambda_{AA}\eta_A) + \frac{\pi}{6}\rho_A\lambda_{AB}R_B R_{AB}^2 \right)^2 \right]. \tag{19}$$

Here, $\Delta = (1-\lambda_{AA}\eta_A)(1-\lambda_{BB}\eta_B) - \eta_A\eta_B\lambda_{AB}^2 R_{AB}^4/R_A^2R_B^2$, where $\eta_i = \frac{1}{6}\pi\rho_i R_i^3$ represents the volume fraction of species i in the system, and $x_i = \rho_i/\Sigma_k \rho_k$. Note that the result for S, given by equation (19), is not restricted to the system considered here but that it holds for any two-component mixture of adhesive hard spheres. In the present case, in which $\lambda_{AB} = 0$, (19) can be simplified to give

$$\begin{aligned} S &= x_A S_{AA} + x_B S_{BB} \\ &= \frac{x_A}{(1-\lambda_{AA}\eta_A)^2} + \frac{x_B}{(1-\lambda_{BB}\eta_B)^2}. \end{aligned} \tag{20}$$

The quantities S_{AA} and S_{BB} denote the average size of clusters formed by particles of species A and B, respectively. Percolation occurs (i.e. $S \to \infty$) when either S_{AA} or S_{BB} diverges. These conditions, respectively, correspond to

$$\lambda_{AA}\eta_A = 1 \tag{21a}$$

or

$$\lambda_{BB}\eta_B = 1. \tag{21b}$$

Using (11) to eliminate λ_{AA} from (21a) yields the threshold for the percolation of species A

$$\tau_{AA} = \frac{(1-\xi_3)^2 + 18\eta_A\xi_2 R_A}{12(1-\xi_3)^2}. \tag{22}$$

Similarly, the percolation locus of species B is found to be

$$\tau_{BB} = \frac{(1-\xi_3)^2 + 18\eta_B\xi_2 R_B}{12(1-\xi_3)^2}. \tag{23}$$

Equations (22) and (23) give the percolation temperature at which clusters of infinite size are formed by particles of species A and B, respectively. Note that the value of

τ_{AA} required for percolation of species A is independent of whether species B is percolating or not, and vice versa. When both percolation conditions are simultaneously satisfied, the system possesses two interpenetrating infinite aggregates or 'gels'.

4. Results and discussion

We first examine the effect of the presence of species B on the clustering of species A. This effect can be seen in figure 1, in which the root λ_{AA}, which determines the extent of A-A aggregation, is plotted as a function of the dimensionless density ρ_B^* $(=(\pi/6)\rho_B R_A^3)$ for a fixed value of ρ_A^* $(=(\pi/6)\rho_A R_A^3) = 0.1$, $R_B/R_A = 1$, and different values of τ_{AA}. Note that, at a given ρ_B^*, λ_{AA} increases with decreasing τ_{AA}. This is expected since the effective attraction is stronger at a lower temperature. Also, it is observed that λ_{AA} increases with increasing ρ_B^*. As a consequence of the repulsion between unlike species, the addition of type-B particles enhances the clustering of A particles. This steric repulsion effect should be more evident for $R_B > R_A$. Displayed in figure 2 is a plot of λ_{AA} as a function of ρ_B^* for $\tau_{AA} = 0.8$, $\rho_A^* = 0.1$ and various particle-size ratios. This figure indeed shows that, for a fixed reduced density of the *second component*, ρ_B^*, λ_{AA} increases with R_B/R_A. The other root, λ_{BB}, which determines the extent of B-B aggregation, is plotted in figure 3 as a function of ρ_B^* for $\rho_A^* = 0.1$, $R_B/R_A = 1$ and different values of τ_{BB}. As expected, λ_{BB} increases as the density of B particles is increased and it decreases with increasing τ_{BB}, the effective temperature. The effect of the particle-size ratio on λ_{BB} is shown in figure 4.

The average sizes of clusters formed by particles A and B are displayed in figure 5. In this figure, the full and broken curves represent S_{AA} and S_{BB} computed for $\tau_{AA} = \tau_{BB} = 0.4$ and $R_B/R_A = 1.0$. For each S_{ii}, the lower and upper curves are computed for $\rho_A^* = 0.1$ and 0.2, respectively. Both S_{AA} and S_{BB} increase with ρ_B^*. Displayed in

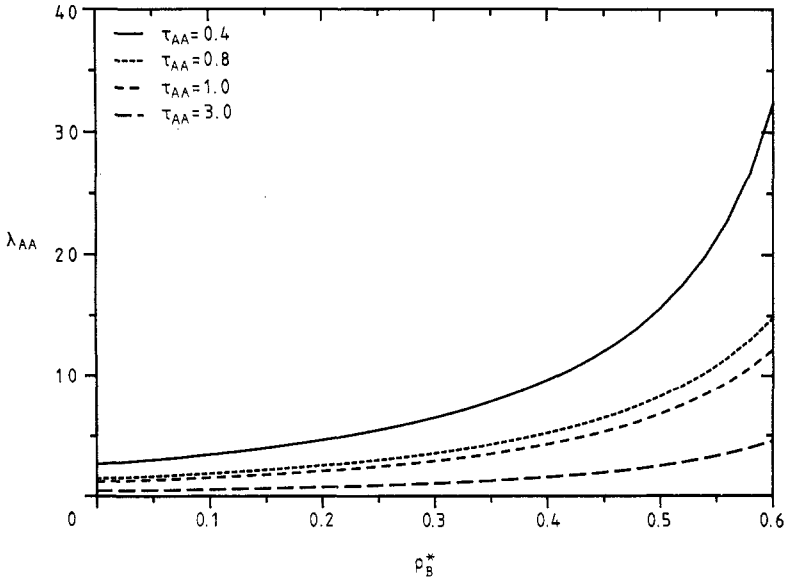

Figure 1. The parameter λ_{AA} plotted as a function of ρ_B^* for $\rho_A^* = 0.1$, $R_B/R_A = 1$, and different values of τ_{AA}.

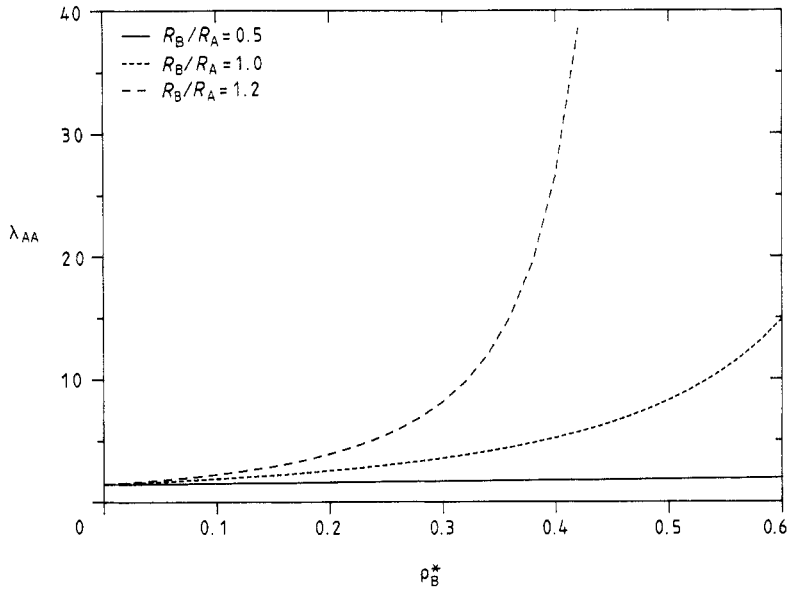

Figure 2. The parameter λ_{AA} plotted as a function of ρ_B^* for $\rho_A^* = 0.1$, $\tau_{AA} = 0.8$, and different values of R_B/R_A.

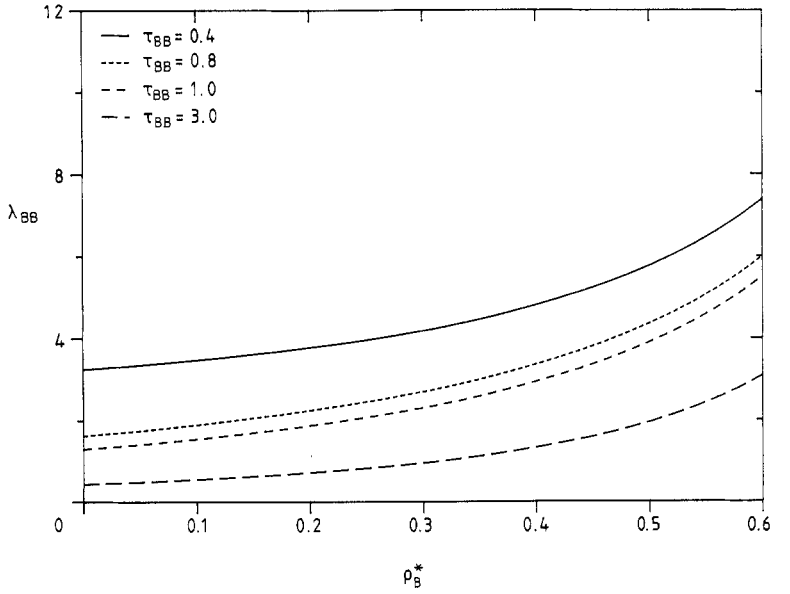

Figure 3. The parameter λ_{BB} plotted as a function of ρ_B^* for $\rho_A^* = 0.1$, $R_B/R_A = 1$, and different values of τ_{AA}.

figure 6 are the percolation temperatures τ_{AA} plotted against ρ_B^* for $\rho_A^* = 0.1$, $\beta = \tau_{BB}/\tau_{AA} = 1$, and various values of particle-size ratios. For each set of curves, the lower, intermediate and larger curves correspond to $R_B/R_A = 1.2$, 1.0 and 0.5 respectively.

In addition to the mean cluster size and the percolation temperature, we have also obtained the pair-connectedness function $g_{ii}^{+}(r)$. For the AHS mixture considered here,

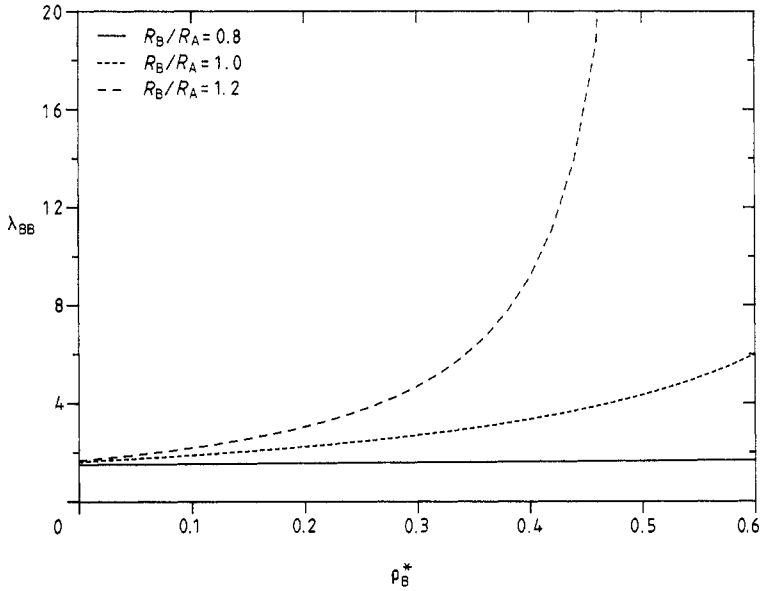

Figure 4. The parameter λ_{BB} plotted as a function of ρ_B^* for $\rho_A^* = 0.1$, $\tau_{AA} = 0.8$, and different values of R_B/R_A.

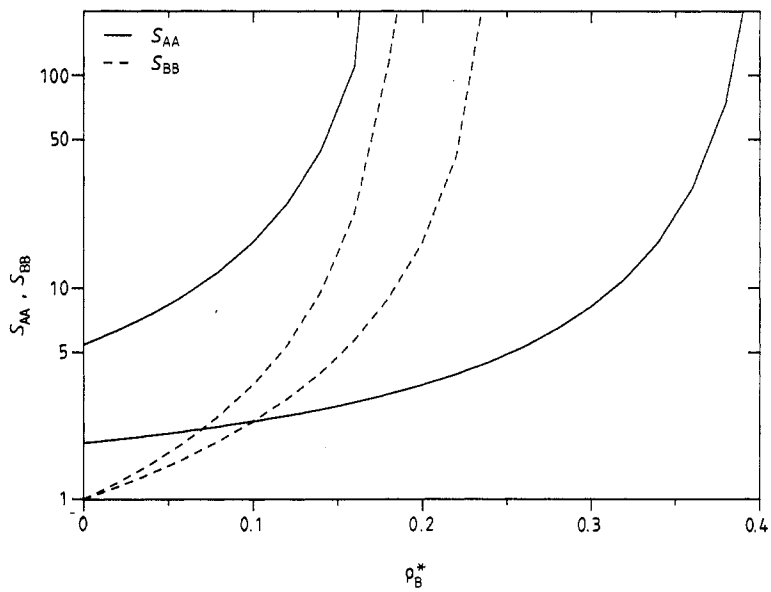

Figure 5. The mean cluster sizes S_{AA} and S_{BB} plotted as a function of ρ_B^* for $R_B/R_A = 1$ and $\tau_{AA} = \tau_{BB} = 0.4$. For each set of S_{ii}, the upper and lower curves correspond to $\rho_A^* = 0.2$ and 0.1, respectively.

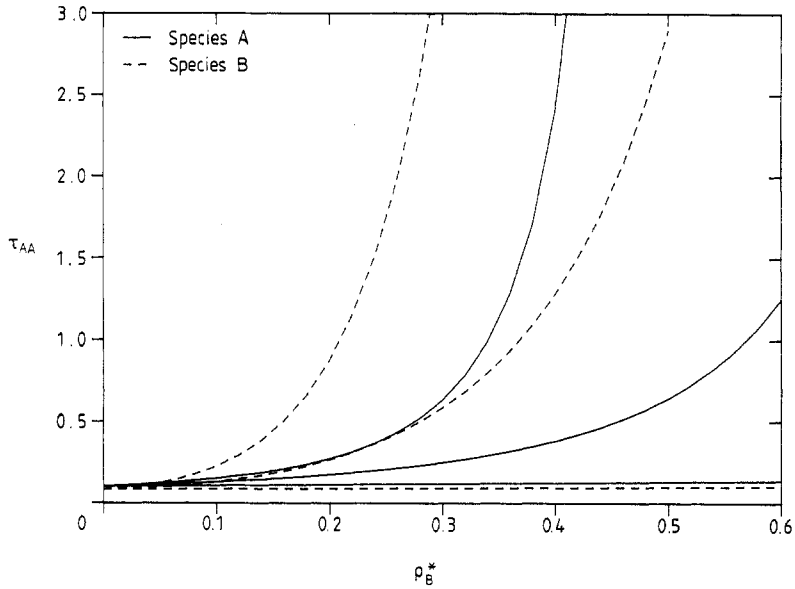

Figure 6. The percolation temperatures of species A (τ_{AA}) and species B (τ_{BB}) plotted as a function of ρ_B^* for $\rho_A^* = 0.1$, $\beta = \tau_{BB}/\tau_{AA} = 1$, and $R_B/R_A = 0.5$ (lower), 1.2 (intermediate), and 1.5 (upper).

the function $g_{ii}^+(r)$ can be determined analytically by transforming (12) into a delay-differential equation (Bellman and Cooke 1963, Chiew and Stell 1985). If we let $f_{ii}(r) = rg_{ii}^+(r)$, (12) becomes

$$f_{ii}(r) = 2\pi \sum_k \rho_k \int_{S_{ij}}^{R_{ij}} \mathrm{d}t\, q_{ik}(t) f_{ik}(r-t). \tag{24}$$

Since $q_{ik}(t) = 0$ for $i \neq k$, (24) simplifies to

$$f_{ii}(r) = 2\pi\rho_i \int_0^{R_{ii}} \mathrm{d}t\, q_{ii}(t) f_{ii}(r-t). \tag{25}$$

Differentiating (25) with respect to r yields the following delay-differential equation:

$$f'_{ii}(r) - 2\pi\rho_i q_{ii}(0) f_{ii}(r) = -\tfrac{1}{6}\pi\rho_i \lambda_{ii} R_{ii}^2 f_{ii}(r - R_{ii}). \tag{26}$$

Equation (26) is a first-order inhomogeneous ordinary differential equation. The function $f_{ii}(r)$ can be determined if $f_{ii}(r - R_{ii})$ is known, which is the case here. If we substitute (9*a*) into (26), we find that, for $R_{ii} < r < 2R_{ii}$,

$$f'_{ii}(x) - z_i f_{ii}(x) = -\zeta_i \delta(x-2) \tag{27}$$

where $x = r/R_{ii}$, $z_i = \lambda_{ii}\eta_i$ and $\zeta_i = \lambda_{ii} z_i$. The presence of the delta function in (27) implies that $f_{ii}(x)$ is discontinuous at $x = 2$. It is straightforward to solve (27) to obtain

$$f_{ii}(x) = \zeta_i \exp[z_i(x-1)] \qquad \text{for } 1 < x < 2. \tag{28}$$

If the above procedure is carried out recursively for the ranges $2 < x < 3$ and $3 < x < 4$, we find that, for $2 < x < 3$,

$$f_{ii}(x) = \zeta_i \exp[z_i(x-2)][\exp(z_i) - 1 - z_i(x-2)] \tag{29}$$

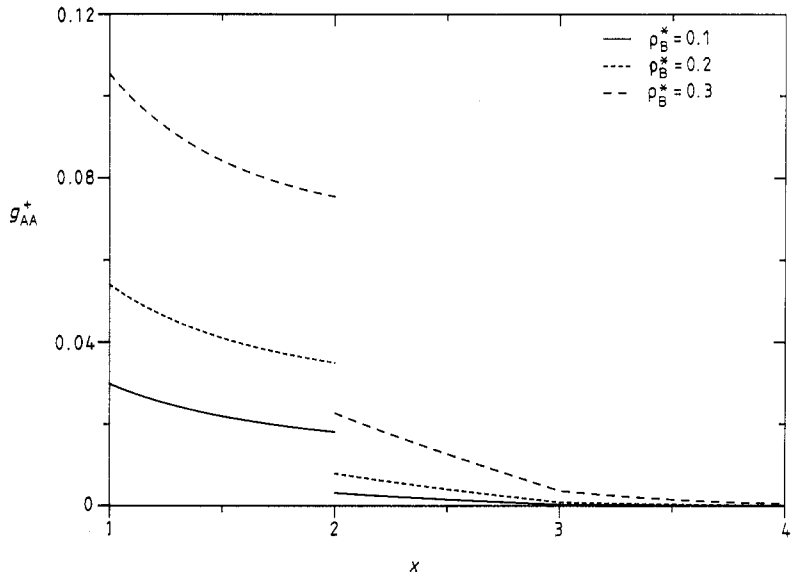

Figure 7. Pair-connectedness function g^+_{AA} plotted as a function of x for $\rho^*_A = 0.1$, $R_B/R_A = 1$, and different values of ρ^*_B.

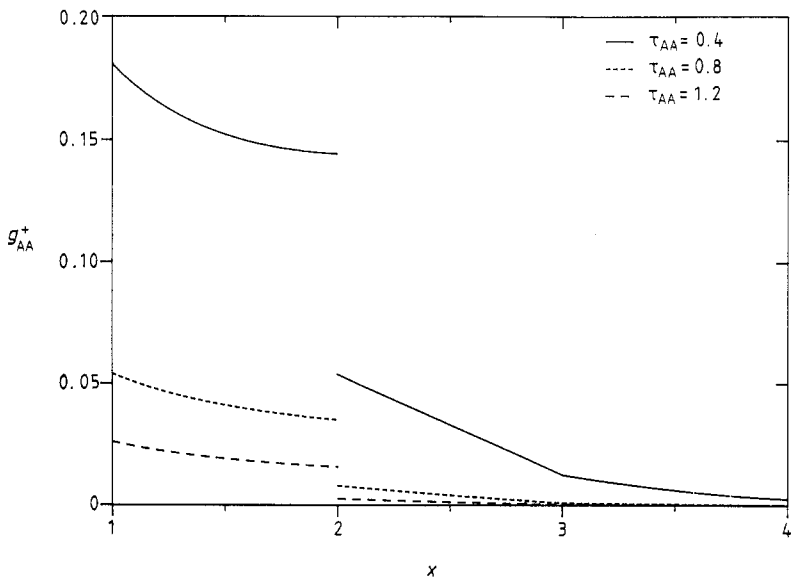

Figure 8. Pair-connectedness function g^+_{AA} plotted as a function of x for $\rho^*_A = 0.1$, $\rho^*_B = 0.2$, $R_B/R_A = 1$ and different values of τ_{AA}.

and, for $3 < x < 4$,

$$f_{ii}(x) = \zeta_i \exp[z_i(x-3)] \times \{\exp(z_i)[\exp(z_i) - 1 - z_i(x-2)] + z_i(x-3)[1 + z_i(x-3)/2]\}. \quad (30)$$

The pair-connectedness function $g^{+}_{AA}(x)$ $(=f^{(x)}_{AA}/x)$ plotted as a function of the dimensionless distance $x\,(=r/R_{AA})$, for $R_B/R_A = 1.0$, $\rho^*_A = 0.1$ and different values of ρ^*_B, is shown in figure 7. The function $g^{+}_{AA}(x)$ is discontinuous at $x = 2$, and decreases with x. An inspection of the figure shows that, for a given x, $g^{+}_{AA}(x)$ increases with increasing ρ^*_B. This is in agreement with our previous observation that the addition of B particles promotes the clustering of A. Plotted in figure 8 is $g^{+}_{AA}(x)$ for $\rho^*_A = 0.1$, $\rho^*_B = 0.2$, $R_B/R_A = 1.0$ and different values of τ_{AA}.

At the percolation threshold, $z_{ii} = \lambda_{ii}\eta_i = 1$ (i.e. equation (21)). This implies that $\zeta_i = \frac{1}{12}\lambda_{ii} = (12\eta_i)^{-1}$. Combining this result with the analytic expressions for $g^{+}_{ii}(x)$, i.e. (28)-(30), reveals that the function $[\eta_i f_{ii}(x)]_{perc}$ is independent of τ_{ii}. This means that, *at the percolation threshold*, $\eta_i f_{ii}(x)$ for different temperatures all collapse into a single curve. This interesting result holds only in the PY approximation, and is not expected to be valid in general.

Acknowledgments

YCC acknowledges the support of the Petroleum Research Fund administered by the American Chemical Society. EDG is grateful for support by the Gas Research Institute.

References

Baxter R J 1968a *Aust. J. Phys.* **21** 563
—— 1968b *J. Chem. Phys.* **49** 2770
—— 1970 *J. Chem. Phys.* **52** 4559
Bellman R E and Cooke K L 1963 *Differential-Difference Equations* (New York: Academic)
Bhattacharya S, Stokes J P, Kim M W and Huang J S 1985 *Phys. Rev. Lett.* **55** 1884
Bug A L R, Safran S A, Grest G S and Webman 1985 *Phys. Rev. Lett.* **55** 1896
Cazabat A M, Chateney D, Geuring P, Langevin D, Meunier J and Sorba O 1984 *Surfactants in Solution* ed K L Mittal and B Lindeman (New York: Plenum) p1737
Chiew Y C and Glandt E D 1983 *J. Phys. A: Math. Gen.* **16** 2599
Chiew Y C and Stell G 1985 *Report #461 SUNY College of Engineering*
Chiew Y C, Stell G and Glandt E D 1985 *J. Chem. Phys.* **83** 761
Chiew Y C and Wang Y H 1988 *J. Chem. Phys.* **89** 6385
Coniglio A, DeAngelis U and Forlani A 1977 *J. Phys. A: Math. Gen* **10** 1123
Cummings P T, Perram J W and Smith E R 1976 *Mol. Phys.* **31** 535
DeSimone T, Demonlini S and Stratt R M 1985 *J. Chem. Phys.* **85** 391
Hill T L 1955 *J. Chem. Phys.* **23** 617
Huang J S, Safran S A, Kim M W, Grest G S, Kotlarchyk M and Quirke N 1984 *Phys. Rev. Lett.* **53** 592
Kim M W and Huang J S 1986 *Phys. Rev.* A **34** 719
Netemeyer S C and Glandt E D 1986 *J. Chem. Phys.* **85** 6054
Perram J W and Smith E R 1977 *Proc. R. Soc.* A **353** 193
Safran S A, Webman I and Grest G S 1985 *Phys. Rev.* A **32** 506
Stell G 1984 *J. Phys. A: Math. Gen.* **17** L855
Wu G H and Chiew Y C 1989 *J. Chem. Phys.* **90** 5024